Adversarial Image Translation: Unrestricted Adversarial Examples in Face Recognition Systems

Kazuya Kakizaki[1] **and Kosuke Yoshida**[1*]
[1]NEC Corporation
7-1, Shiba 5-chome Minato-ku, Tokyo 108-8001 Japan
kazuya1210@nec.com, dep58@nec.com

Abstract

Thanks to recent advances in deep neural networks (DNNs), face recognition systems have become highly accurate in classifying a large number of face images. However, recent studies have found that DNNs could be vulnerable to adversarial examples, raising concerns about the robustness of such systems. Adversarial examples that are not restricted to small perturbations could be more serious since conventional certified defenses might be ineffective against them. To shed light on the vulnerability to such adversarial examples, we propose a flexible and efficient method for generating unrestricted adversarial examples using image translation techniques. Our method enables us to translate a source image into any desired facial appearance with large perturbations to deceive target face recognition systems. Our experimental results indicate that our method achieved about 90 and 80% attack success rates under white- and black-box settings, respectively, and that the translated images are perceptually realistic and maintain the identifiability of the individual while the perturbations are large enough to bypass certified defenses.

Introduction

Deep neural networks (DNNs) have become more accurate than humans in image classification (Krizhevsky, Sutskever, and Hinton 2012) and machine translation (Bahdanau, Cho, and Bengio 2014). However, recent studies have shown that DNNs could be vulnerable to adversarial examples (Szegedy et al. 2014; Goodfellow, Shlens, and Szegedy 2015; Carlini and Wagner 2017). Specifically, DNNs could be intentionally deceived by an input data point that has been slightly modified. To understand the mechanism of such a vulnerability and make DNNs more robust, it is important to study methods for generating adversarial examples.

The vulnerability to adversarial examples raises concerns about face recognition systems widely used in applications such as biometric authentication and public safety (Masi et al. 2018). Since the recent success of face recognition systems rely on DNNs, a potential attacker could exploit adversarial examples for incorrect recognition or impersonating another person. Therefore, it is important to consider the risk of adversarial examples attacking face recognition systems.

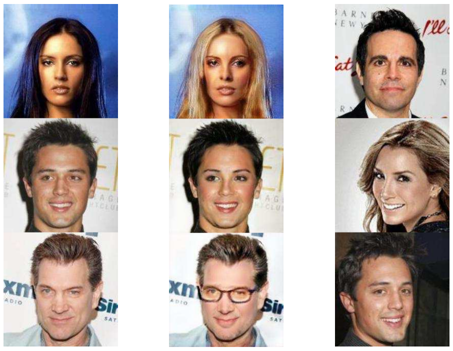

Figure 1: Adversarial image translation against face recognition systems. Our method translates (a) original images into (b) adversarial images with desired domain labels to classify them as (c) target images. Corresponding domain labels are blond hair, makeup, and eyeglasses from top to bottom.

Typical methods for creating adversarial examples for deceiving target classifiers involve adding small carefully crafted perturbations on a source image (Szegedy et al. 2014; Goodfellow, Shlens, and Szegedy 2015; Carlini and Wagner 2017). To reduce the risk of adversarial examples based on small perturbations, several defenses have been proposed with theoretical certification. These defenses provide a lower bound of class-changing perturbations based on the global Lipschitz constant of DNNs (Cisse et al. 2017; Gouk et al. 2018; Tsuzuku, Sato, and Sugiyama 2018) and randomized smoothing (Li et al. 2018; Cohen, Rosenfeld, and Kolter 2019; Lecuyer et al. 2019). These studies indicate that small-perturbation-based attacks may no longer be effective with these defenses.

In spite of these certified defenses, there remains a significant risk of adversarial examples. Song et al. and Brown et al. independently introduced a novel concept called unrestricted adversarial examples (Song et al. 2018; Brown et al. 2018). While such adversarial examples are not restricted to small perturbations, they do not confuse human observers. For instance, an image of a stop sign is still recognized as a

[*] both authors contributed equally

stop sign by human observers, though the adversarial perturbations are large enough to bypass certified defenses. These adversarial examples could be a serious security issue and shed light on the mechanism of this type of vulnerability.

In the context of face recognition systems, how can we define unrestricted adversarial examples in a reasonable scenario? Spatial transformation, such as adversarial rotation (Brown et al. 2018) and distortion (Goswami et al. 2018), are impractical for attacks against face recognition systems since adversaries are unable to control the spatial transformations in biometric authentication and public surveillance (e.g. rotated images cannot be presented in a passport-control scenario). Therefore, we focus on unrestricted adversarial examples without spatial transformation. We consider the following conditions: our adversarial examples (1) should be perceptually realistic enough to maintain the identifiability of the individual in the original image and (2) have large enough perturbations to bypass defenses that are based on small perturbations.

To generate unrestricted adversarial examples that satisfy these two conditions, we propose a method that takes advantage of recent image translation techniques into different domains (Choi et al. 2018). Our method enables us to translate the facial appearance in a source image into several domains so that face recognition systems can be deceived. While the translation provides perceptible perturbations on the face, it avoids damaging the identifiability of the individual of the source for human observers.

Figure 1 illustrates the flow of our method: (a) the original images are translated into (b) adversarial images with respect to several domains to be classified as (c) the target images. From top to bottom, we translate in three different domain labels: blond hair, makeup, and eyeglasses. They show that changing hair-color and adding face accessories, such as makeup and eyeglasses, deceive face recognition systems. Translating a given image into any desired facial appearance in this way enables us to evaluate the risk of diverse unrestricted adversarial examples.

In our experiments, we found that our method achieved about 90% attack success rate on average against publically available face recognition models in VGGFace and its latest version VGGFace2. Our method can also generate realistic adversarial images with the desired facial appearance and maintain the identifiability of the individual even with large perturbations. We applied our method to a black-box setting and evaluated black-box attacks based on the transferability phenomenon and dynamic distillation strategy (Szegedy et al. 2014; Xiao et al. 2018).

Our contributions are listed as follows.

- We propose a flexible and efficient method for generating unrestricted adversarial examples against face recognition systems.
- We confirm that the generated adversarial examples are perceptually realistic enough to maintain the identifiability of the individual to avoid confusing human observers.
- We experimentally demonstrated that our method can deceive face recognition systems with high attack success rates under white- and black-box settings.
- We confirm that generated adversarial examples bypass a state-of-the-art certified defense.

This paper is organized as follows. In Section 2, we review related studies on image translation methods based on generative adversarial networks (GANs) and adversarial examples in face recognition systems. In Section 3, we provide details of our proposed method. In Section 4, we report the settings and results of our experiments. We conclude this paper in Section 5.

Related Studies

In this section, we review several related studies on unrestricted adversarial examples, GANs, and adversarial face accessories.

Unrestricted Adversarial Examples

Song et al. proposed a method for generating unrestricted adversarial examples from scratch instead of adding small perturbations on a source image and demonstrated that their generated examples successfully bypassed several certified defenses that are based on small perturbations (Song et al. 2018). They adopted two classifiers: a target classifier that they wish to deceive and an auxiliary classifier that provides correct predictions. These classifiers encourage the examples generated from scratch to deceive the target classifier without changing any semantics. They confirmed that their method successfully created unrestricted adversarial examples without confusing human observers by using Amazon Mechanical Turk (AMTurk). While their work is notable, more effort is required to deceive face recognition systems.

Generative Adversarial Networks (GANs)

GANs have achieved significant results especially in image generation tasks (Goodfellow et al. 2014; Karras et al. 2018; Karras, Laine, and Aila 2018). They consist of two components: a generator and discriminator. The generator is trained to provide fake images that are indistinguishable from real ones by the discriminator, while the discriminator is trained to distinguish fake images from real images. This competitive setting is represented by an adversarial loss.

Xiao et al. proposed a method for exploiting GANs to generate realistic adversarial images (Xiao et al. 2018). With their method, the generator is trained to provide adversarial images that are indistinguishable from real ones by the discriminator. They demonstrated that their generated adversarial examples were perceptually realistic through human evaluation. The generator also efficiently provides adversarial examples once it is trained. This could be beneficial to potentially improve the robustness of target models.

Choi et al. introduced a framework called StarGAN that enables us to translate an input image into multiple domains using GANs (Choi et al. 2018). In addition to conventional GANs, they introduced two loss functions: auxiliary classification loss and reconstruction loss. The first one is to guarantee that the output image can be classified into the corresponding domain label (Odena, Olah, and Shlens 2017). The second one is to preserve the content of the input image in the translated image as cycle consistency loss (Zhu et al. 2017) since StarGAN formulation consists of only a single generator. They demonstrated that StarGAN is useful in translating face images into any desired domain or facial expression in a flexible manner.

Deceiving Face Recognition Systems

Some studies modified the facial appearances of source images by adding adversarial face accessories and deceived face recognition systems for the purpose of impersonation or privacy preservation (Sharif et al. 2016; 2017; Feng and Prabhakaran 2013). For instance, Sharif et al. created adversarial eyeglasses by iteratively updating their color. These eyeglasses allow adversaries to impersonate another person with high success rates in several state-of-the-art face recognition systems. While these studies demonstrated the significant risk of adversarial examples, they have limited scalability to understand the mechanism of such vulnerability.

We take advantage of recent studies on image translation with GANs to translate the facial appearance of source images in an adversarial manner. This translation introduces large perturbations on the source images; therefore, translated images are unrestricted adversarial examples against face recognition systems.

Our Method

We first provide problem definitions and notations for our method then introduce our formulation to translate hair color, makeup, and eyeglasses of a peoples facial images so that the target face recognition models can be deceived from the impersonation of others.

Problem Definition

Given an instance (x_i, y_i, c_i), which is composed of a face image $x_i \in \mathcal{X}$ sampled according to some unknown distribution, class label $y_i \in \mathcal{Y}$ corresponding to the person of the image, and domain label c_i representing the existence of each binary domain. Here, c_i is a binary vector whose j-th component is 1 when the corresponding image exhibits the j-th binary domain. The target face recognition models learn a classifier $\phi : \mathcal{X} \rightarrow \mathcal{Y}$ that assigns class labels into each face image. Our objective is to generate adversarial example $\hat{x_i}$ classified as $\phi(\hat{x_i}) = t(t \neq y_i)$, where t is our target class label. In addition, $\hat{x_i}$ should have the desired domain label.

Formulation

Our method is mainly based on a framework of recent GANs and consists of four components: a generator G, discriminator D_s, auxiliary classifier D_c, and target model ϕ. The G provides images indistinguishable for the D by optimizing an adversarial loss L_{wgan}. The generated images are encouraged to have any desired domain label by minimizing a classification loss L^r_{cla}, L^f_{cla}. The target loss L_{tar} is minimized to deceive the target models (i.e. face recognition systems) through impersonation.

Adopted from StarGAN (Choi et al. 2018), we train a single G to translate input face images into output images with any desired domain label. The G takes a face image x and a desired domain label c_{out} as an input and generates an output image $\hat{x}$ whose domain label is c_{out}, $G : x, c_{out} \rightarrow \hat{x}$. The D_s takes $\hat{x}$ and provides a probability distribution over sources, $D_s(\hat{x})$. The goal with these components is to optimize the adversarial loss defined as

$$L_{gan} = E_x[\log D_s(x)] + E_x[\log(1 - D_s(G(x, c_{out})))], \quad (1)$$

where the G attempts to minimize the loss while the D_s attempts to maximize it to generate realistic images.

To take advantage of recent techniques for stabilizing GAN training, we adopt the Wasserstein GAN with gradient penalty (Gulrajani et al. 2017) defined as

$$\begin{aligned} L_{wgan} \quad = \quad & E_x[D_s(x)] + E_x[(1 - D_s(G(x, c_{out})))] \\ & - \lambda_{wgan} L_{pen}, \end{aligned} \quad (2)$$

where λ_{wgan} represents a hyper parameter that controls the magnitude of the penalty term L_{pen}. To enforce the Lipschitz constant, the penalty term is defined as

$$L_{pen} = E_x[(\|\nabla_{x_q} D_s(x_q)\|_2 - 1)^2], \quad (3)$$

where x_q is sampled uniformly along straight lines between real and generated images. We set λ_{wgan} to 10.

To encourage the generated image to have the desired domain label c_{out}, we adopt the auxiliary classification loss (Odena, Olah, and Shlens 2017). Specifically, we optimize the D_c to classify the real images as corresponding domain labels by minimizing the loss, which is defined as

$$L^r_{cla} = E_{x, c_{in}}[-\log D_c(c_{in}|x)], \quad (4)$$

where $D_c(c_{in}|x)$ represents a probability distribution over the domain labels and c_{in} corresponds to the domain label of an input. We then optimize the G to classify the generated images as any target domain label by minimizing the loss, which is defined as

$$L^f_{cla} = E_{x, c_{out}}[-\log D_c(c_{out}|G(x, c_{out}))]. \quad (5)$$

Adopted from a common practice of image translation to maintain the identifiability of the individual (Zhu et al. 2017), we add reconstruction loss, which is defined as

$$L_{rec} = E_{x, c_{out}, c_{in}}[\|x - G(G(x, c_{out}), c_{in})\|_1]. \quad (6)$$

Note we adopt L1 norm to obtain less blurring images.

We add loss to encourage a target model ϕ to classify the generated images as target labels t. This loss is defined as

$$L_{tar} = E_x[\max(\max_{i \neq t} z_i(x) - z_t(x), \kappa)], \quad (7)$$

where z is the output of ϕ except the final softmax layer (i.e. logits) and κ is a hyper parameter set to negative values in our experiments.

Finally, our full loss function is defined as

$$\begin{aligned} L_G \quad &= \quad L_{wgan} + \lambda_\alpha L^f_{cla} + \lambda_\beta L_{rec} + \lambda_\gamma L_{tar}, \quad (8) \\ L_D \quad &= \quad -L_{wgan} + \lambda_\alpha L^r_{cla}, \quad (9) \end{aligned}$$

where we obtain our G, D_s, and D_c by minimizing L_G and L_D, respectively. Note λ_α, λ_β, and λ_γ are hyper parameters that control the relative importance of each loss function.

Table 1: Accuracy of target face recognition models on legitimate datasets, evaluated using images held aside for testing. Our target face recognition models achieved high accuracy in all cases. VGG(A) and ResNet(A): VGG16 and ResNet50 for case A. VGG(B) and ResNet(B): VGG16 and ResNet50 for case B. StarGAN: image translation without adversarial effect ($\lambda_\gamma = 0$).

	VGG(A)	ResNet(A)	VGG(B)	ResNet(B)
legitimate	0.97	1.00	0.95	0.96
StarGAN (Choi et al. 2018)	0.85	0.93	0.73	0.75

Table 2: Average, maximum, and minimum attack success rates. Our generated adversarial examples achieved about 90% attack success rate on average against two models with different domain labels.

	hair color (black/blond)				makeup				eyeglasses			
	VGG		ResNet		VGG		ResNet		VGG		ResNet	
	A	B	A	B	A	B	A	B	A	B	A	B
Ave.	0.85	0.98	0.95	0.96	0.83	0.98	0.94	0.96	0.83	0.96	0.93	0.86
Max.	0.95	0.99	1.00	0.98	0.90	0.99	1.00	0.98	0.94	0.98	1.00	0.97
Min.	0.70	0.97	0.75	0.92	0.65	0.96	0.66	0.94	0.74	0.94	0.78	0.50

Experiments Results

We first demonstrated that our method achieves more than a 90% attack success rate against two target models in a white-box setting with high quality images. We then evaluated black-box attacks based on the transferability phenomenon of adversarial examples (Szegedy et al. 2014; Goodfellow, Shlens, and Szegedy 2015; Papernot et al. 2016) and the dynamic distillation strategy (Xiao et al. 2018). Finally, we show that adversarial examples obtained with our method satisfy two conditions: they are (1) realistic enough to maintain the identifiability of the individual and (2) have large perturbations to bypass certified defenses.

Dataset

We used the CelebA dataset, which has 202,599 face images with 40 binary attributes (Liu et al. 2015). To train the target face recognition models, we randomly selected 10 persons as case A and 100 persons as case B. We only used 20 images per person for the training dataset and the rest of the images were held aside for the test dataset.

Target Face Recognition Models

Our target face recognition models were VGGFace (Parkhi, Vedaldi, and Zisserman 2015) and VGGFace2 (Cao et al. 2018). We downloaded publically available pre-trained VGG16 [1] for VGGFace and ResNet50 [2] for VGGFace2. These pre-trained models exhibit state-of-the-art results for face recognition tasks. They take a 224x224 face image as an input and provide a low-dimensional face descriptor in which two images of the same person are designed to be closer to each other.

On top of the pre-trained face descriptor, we constructed a fully connected layer to define our own target face recognition models with the CelebA dataset. We fine-tuned the parameters from the fully connected layer using categorical cross entropy loss with the training dataset. Our fine-tuned models achieved more than 95% accuracy on the test dataset, as shown in Table 1. This table also shows the test accuracy on translated images without any adversarial effect: in which $\lambda_\gamma = 0$ in Equation (8), indicating that the models are robust against simply changing domain labels in StarGAN.

Implementation Details

We adopted a similar architecture from image translation studies (Zhu et al. 2017; Choi et al. 2018). In particular, we constructed two down-sampling blocks, six residual blocks, and two up-sampling blocks with rectified linear unit (ReLU) layers for the G, and five down-sampling blocks with leaky ReLUs and fully connected blocks for the D. We applied PatchGAN (Isola et al. 2017) to construct the D following previous studies.

We trained both models using Adam with $\beta_1 = 0.5$ and $\beta_2 = 0.999$. The learning rate linearly decreased (Choi et al. 2018) and batch size was set to 32 in all experiments. We used $\lambda_\alpha = 1$, $\lambda_\beta = 10$ for L_G and L_D and $\kappa = -0.3$ for L_{tar}. For cases A and B, we set λ_γ to 0.2 and 0.5 and number of epochs to $300,000$ and $500,000$, respectively.

Attacks in White-Box Setting

We first evaluated our method under a white-box setting in which the adversary has access to the model architecture and its weights. Since we chose all individuals as targets of impersonation, we evaluated ten different Gs and Ds for case A. For case B, we randomly chose 5 of the 100 individuals as targets of impersonation. Our evaluation of the attack success rate involved using the test dataset held aside from training of our models for fair evaluation.

Theoretically, we can apply 40 types of domain labels available in the CelebA dataset. However, we only applied three domain labels: hair color (black/blond), heavy makeup, and eyeglasses since our goal was to efficiently generate images in practical scenarios for attacking face

[1] https://github.com/yzhang559/vgg-face

[2] https://github.com/rcmalli/keras-vggface

recognition systems (Sharif et al. 2016; 2017; Feng and Prabhakaran 2013).

We report the average, maximum, and minimum attack success rates among different models in both cases. Table 2 shows that our method achieved high attack success rates in both models and domain labels. From the performance results in Table 2, we can see that about 90% of test images could be successful in deceiving our target face recognition models by changing their facial appearance.

Figure 3 illustrates successful adversarial examples. The left columns show the original images and middle ones show the adversarial examples with several domain labels: blond/black hair, makeup, and eyeglass from top to bottom. The target images that we tried to impersonate are presented in the right columns. These images demonstrate that our method accurately translates source images into multiple domains, enabling the target face recognition models to be deceived. Moreover, the introduced perturbations are perceptible to human observers while avoiding the damages in the identifiability of the individual of the source images.

Attacks in Black-Box Setting

Since most face recognition systems do not allow anyone to acquire knowledge about their network architectures and weights, it is important to analyze vulnerabilities in black-box setting. We explored the attack strategies based on the transferability phenomenon in which adversarial examples generated in a model will also lead to successful attacks against other models (Szegedy et al. 2014; Goodfellow, Shlens, and Szegedy 2015; Papernot et al. 2016). We generated adversarial images with one target face recognition model and evaluated the attack success rates against another model.

Table 3 lists the results of transferability-based attacks between the two target face recognition models: VGG16 and ResNet50. We found that about 30% of attacks transferred from VGG16 to ResNet50, and vice versa. These results indicate that publically available face recognition systems are vulnerable to simple transferability-based attacks even without any knowledge about the models.

We also evaluated our method based on the dynamic distillation strategy in a black-box setting (Xiao et al. 2018). This enables us to obtain a distilled model that behaves similar to a black-box model. As described in previous studies, we repeated the following two steps in each iteration.

First step. Update the distilled model $\hat{\phi}$ with a fixed G and D by minimizing the following objectives:

$$E_x[H(\hat{\phi}(x), b(x))] + E_x[H(\hat{\phi}(G(x, c_{out})), b(G(x, c_{out}))] \tag{10}$$

where H denotes the cross-entropy loss and $\hat{\phi}(x)$ and $b(x)$ denote the output of the distilled model and black-box model, respectively. This step encourages the distilled model to behave similar to the target black-box model on generated adversarial examples.

Second step. Update our G and D with $\hat{\phi}$ using Equations (8) and (9). In this step, we can uses our method on the distilled models, as described in a white-box setting.

Table 4 shows that with the dynamic distillation, our method achieved a more than 80% attack success rate for VGG16 and about 70% for ResNet50 on average with $200,000$ epochs. These results indicate that the dynamic distillation strategy is beneficial for our method in a black-box setting. Note that we only discuss the evaluation of the dynamic distillation for case B due to time constraints.

Human Perceptual Study

We evaluated the quality of the images generated with our method using AMTurk to confirm that the images satisfy condition (1): they should be perceptually realistic enough to maintain the identifiability of the individual as an original image. We selected 100 pairs of original and adversarial images and asked workers the question, Do the two images have the same personal identity? Note we assigned each pair to five different workers for fair comparison. For this question, 76.6% of workers answered that personal identities in the original and adversarial images were the same. This result indicates that our method successfully translates images while maintaining the identifiability of the individual to avoid confusing human observers.

A Comparison between Perturbations and Certified Radius

To meet condition (2): our adversarial examples have large enough perturbations to bypass defenses based on small perturbations, we evaluated a state-of-the-art certified defense with randomized smoothing (Cohen, Rosenfeld, and Kolter 2019). This defense provides certified regions where the classifier has constant output around each data point.

Setup. We constructed smoothed target face recognition model $\tilde{\phi}$ that return the most likely class when x is perturbed as follows:

$$\tilde{\phi} = \text{argmax}_{y \in \mathcal{Y}} P(\phi(x + \epsilon) = y), \tag{11}$$

where ϵ is Gaussian noise with the standard deviation σ and ϕ is a base classifier trained with Gaussian data augmentation (Lecuyer et al. 2019).

To compute the certified regions, we used Cohen's method with $n_0 = 100, n = 1000$, and $\alpha = 0.001$ (Cohen, Rosenfeld, and Kolter 2019). Each certified region is represented by its radius. The ball centered at each image with the radius is guaranteed to have constant output inside the ball.

We used VGG16 and ResNet50 trained with Gaussian data augmentation as the base classifiers for case A. The models were set to publically available pre-trained parameters as initial parameters and trained using stochastic gradient descent with 1000 epochs. We set the learning rate and momentum to 0.0001 and 0.9, respectively.

Result. Figure 2 shows the certified accuracy of our smoothed target face recognition models with radius threshold T. The certified accuracy represents the proportion of images classified correctly and whose certified radius is less than T for all images. In both VGG16 (left) and ResNet50 (right), all certified radii were less than 630. We calculated the average perturbations of our method in L2. The average

Table 3: Average attack success rates in transferability-based attacks between two target face recognition models. About 30% of attacks transferred from VGG16 to ResNet50, and vice versa.

Model	Domain	VGG(A/B)	ResNet(A/B)
VGG(A/B)	hair color	-	0.26/0.28
	makeup	-	0.22/0.33
	eyeglasses	-	0.27/0.36
ResNet(A/B)	hair color	0.35/0.32	-
	makeup	0.29/0.30	-
	eyeglasses	0.22/0.38	-

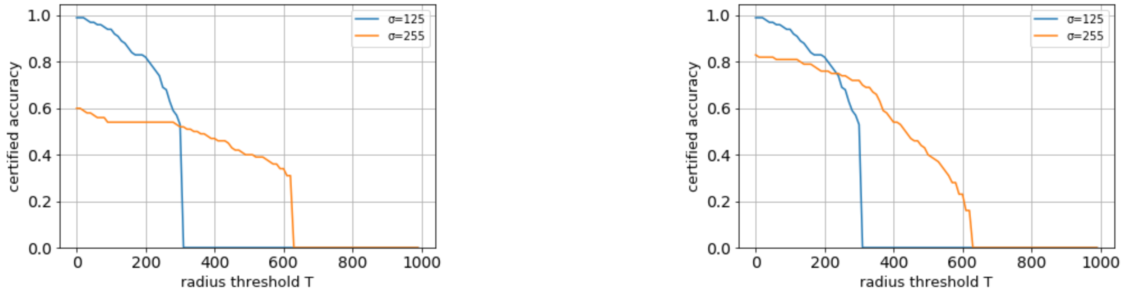

VGG(A)

ResNet(A)

Figure 2: Certified accuracy and radius threshold T for VGG(A) (left) and ResNet(A) (right). Horizontal axis represents T and vertical axis represents certified accuracy: proportion of images classified correctly and whose certified radius is less than T. In both settings, $\sigma = 125$ and 255 respectively, and certified radii were much less than perturbations introduced with our method.

Table 4: Average attack success rates in dynamic-distillation-based attacks

Domain	VGG(B)	ResNet(B)
hair color	0.89	0.73
makeup	0.82	0.69
eyeglasses	0.84	0.71

perturbations for VGGFace(A) were 14,739, 461,290,430, and 3,589,136 for hair color, makeup, and eyeglasses, respectively. The average perturbations for ResNet(A) were 15,342, 461,290,700, and 3,589,382 for hair color, makeup, and eyeglasses, respectively. Note all pixels have values ranging from 0 to 255. We confirmed that all the images generated with our method provide larger perturbations than the certified radii.

These results indicate that the state-of-the-art certified defense might be insufficient for our method. This does not mean that the certified defense is broken since the threat model is different from ours.

Conclusion

We proposed a method for generating unrestricted adversarial examples against face recognition systems. The method translates the facial appearance of a source image into multiple domains to deceive target face recognition systems. Through experiments, we demonstrated that our method achieved about a 90% attack success rate in a white-box setting with respect to several domains: hair color, makeups, and eyeglasses. We also evaluated our method in a black-box setting using transferability of adversarial examples and the dynamic distillation strategy, resulting in 30 and 80% attack success rates, respectively. We also demonstrated that perturbations introduced by our method were large enough to bypass a state-of-the-art certified defense, while the translation prevented the damages in the identifiability of the individual of a source image for human observers. We conclude that our method is promising for improving the robustness of face recognition systems.

References

Bahdanau, D.; Cho, K.; and Bengio, Y. 2014. Neural machine translation by jointly learning to align and translate. *arXiv preprint arXiv:1409.0473*.

Brown, T. B.; Carlini, N.; Zhang, C.; Olsson, C.; Christiano, P.; and Goodfellow, I. 2018. Unrestricted adversarial examples. *arXiv preprint arXiv:1809.08352*.

Cao, Q.; Shen, L.; Xie, W.; Parkhi, O. M.; and Zisserman, A. 2018. Vggface2: A dataset for recognising faces across pose and age. In *International Conference on Automatic Face and Gesture Recognition*.

Carlini, N., and Wagner, D. 2017. Towards evaluating the

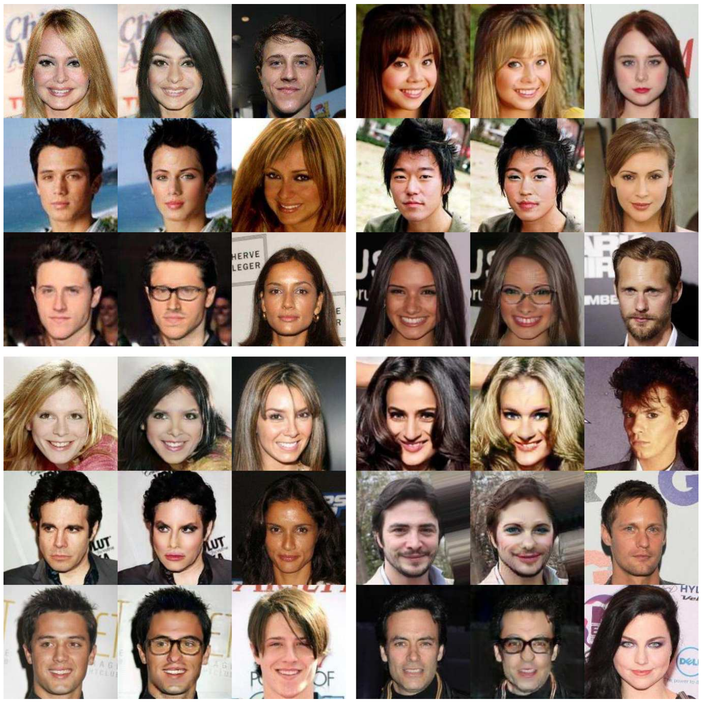

Figure 3: Successful adversarial images. Left columns show original images and middle ones show successful adversarial examples. Corresponding target individuals are presented in right columns. Target domain labels are hair color (black or blond), makeup, and eyeglasses. Introduced perturbations were perceptible while preventing alteration of original identity.

robustness of neural networks. In *Proceedings of the IEEE Symposium on Security and Privacy*, 39–57.

Choi, Y.; Choi, M.; Kim, M.; Ha, J.-W.; Kim, S.; and Choo, J. 2018. Stargan: Unified generative adversarial networks for multi-domain image-to-image translation. In *Proceedings of the IEEE Conference on Computer Vision and Pattern Recognition*, 8789–8797.

Cisse, M.; Bojanowski, P.; Grave, E.; Dauphin, Y.; and Usunier, N. 2017. Parseval networks: Improving robustness to adversarial examples. In *Proceedings of the 34th International Conference on Machine Learning-Volume 70*, 854–863. JMLR. org.

Cohen, J. M.; Rosenfeld, E.; and Kolter, J. Z. 2019. Certified adversarial robustness via randomized smoothing. In *Proceedings of the 36th International Conference on Machine Learning*.

Feng, R., and Prabhakaran, B. 2013. Facilitating fashion camouflage art. In *Proceedings of the 21st ACM international conference on Multimedia*, 793–802.

Goodfellow, I.; Pouget-Abadie, J.; Mirza, M.; Xu, B.; Warde-Farley, D.; Ozair, S.; Courville, A.; and Bengio, Y. 2014. Generative adversarial nets. In *Advances in neural information processing systems*, 2672–2680.

Goodfellow, I.; Shlens, J.; and Szegedy, C. 2015. Explaining and harnessing adversarial examples. In *International Conference on Learning Representations*.

Goswami, G.; Ratha, N.; Agarwal, A.; Singh, R.; and Vatsa, M. 2018. Unravelling robustness of deep learning based face recognition against adversarial attacks. In *Thirty-Second AAAI Conference on Artificial Intelligence*.

Gouk, H.; Frank, E.; Pfahringer, B.; and Cree, M. 2018. Regularisation of neural networks by enforcing lipschitz continuity. *arXiv preprint arXiv:1804.04368*.

Gulrajani, I.; Ahmed, F.; Arjovsky, M.; Dumoulin, V.; and Courville, A. C. 2017. Improved training of wasserstein gans. In *Advances in Neural Information Processing Systems*, 5767–5777.

Isola, P.; Zhu, J.-Y.; Zhou, T.; and Efros, A. A. 2017. Image-to-image translation with conditional adversarial networks. In *2017 IEEE Conference on Computer Vision and Pattern Recognition*, 5967–5976.

Karras, T.; Aila, T.; Laine, S.; and Lehtinen, J. 2018. Progressive growing of gans for improved quality, stability, and variation. In *International Conference on Learning Representations*.

Karras, T.; Laine, S.; and Aila, T. 2018. A style-based generator architecture for generative adversarial networks. *arXiv preprint arXiv:1812.04948*.

Krizhevsky, A.; Sutskever, I.; and Hinton, G. E. 2012. Imagenet classification with deep convolutional neural networks. In *Advances in neural information processing systems*, 1097–1105.

Lecuyer, M.; Atlidakis, V.; Geambasu, R.; Hsu, D.; and Jana, S. 2019. Certified robustness to adversarial examples with differential privacy. In *Proceedings of the IEEE Symposium on Security and Privacy*, 726–742.

Li, B.; Chen, C.; Wang, W.; and Carin, L. 2018. Second-order adversarial attack and certifiable robustness. *arXiv preprint arXiv:1809.03113*.

Liu, Z.; Luo, P.; Wang, X.; and Tang, X. 2015. Deep learning face attributes in the wild. In *Proceedings of International Conference on Computer Vision*.

Masi, I.; Wu, Y.; Hassner, T.; and Natarajan, P. 2018. Deep face recognition: a survey. In *2018 31st SIBGRAPI Conference on Graphics, Patterns and Images*, 471–478.

Odena, A.; Olah, C.; and Shlens, J. 2017. Conditional image synthesis with auxiliary classifier gans. In *Proceedings of the 34th International Conference on Machine Learning*, 2642–2651.

Papernot, N.; McDaniel, P.; Goodfellow, I.; Jha, S.; Celik, Z. B.; and Swami, A. 2016. Practical black-box attacks against deep learning systems using adversarial examples. *arXiv preprint arXiv:1602.02697* 1(2):3.

Parkhi, O. M.; Vedaldi, A.; and Zisserman, A. 2015. Deep face recognition. In *British Machine Vision Conference*.

Sharif, M.; Bhagavatula, S.; Bauer, L.; and Reiter, M. K. 2016. Accessorize to a crime: Real and stealthy attacks on state-of-the-art face recognition. In *Proceedings of the 2016 ACM SIGSAC Conference on Computer and Communications Security*, 1528–1540.

Sharif, M.; Bhagavatula, S.; Bauer, L.; and Reiter, M. K. 2017. Adversarial generative nets: Neural network attacks on state-of-the-art face recognition. *arXiv preprint arXiv:1801.00349*.

Song, Y.; Shu, R.; Kushman, N.; and Ermon, S. 2018. Constructing unrestricted adversarial examples with generative models. In *Advances in Neural Information Processing Systems*. 8322–8333.

Szegedy, C.; Zaremba, W.; Sutskever, I.; Bruna, J.; Erhan, D.; Goodfellow, I. J.; and Fergus, R. 2014. Intriguing properties of neural networks. In *International Conference on Learning Representations*.

Tsuzuku, Y.; Sato, I.; and Sugiyama, M. 2018. Lipschitz-margin training: Scalable certification of perturbation invariance for deep neural networks. In *Advances in Neural Information Processing Systems*. 6542–6551.

Xiao, C.; Li, B.; yan Zhu, J.; He, W.; Liu, M.; and Song, D. 2018. Generating adversarial examples with adversarial networks. In *Proceedings of the Twenty-Seventh International Joint Conference on Artificial Intelligence, IJCAI-18*, 3905–3911.

Zhu, J.-Y.; Park, T.; Isola, P.; and Efros, A. A. 2017. Unpaired image-to-image translation using cycle-consistent adversarial networks. In *IEEE International Conference on Computer Vision*, 2242–2251.